

***Ab initio* calculation of the electronic, structural, and dynamical properties of Zn-based semiconductors**

Bal K. Agrawal, P. S. Yadav, and Savitri Agrawal

Physics Department, Allahabad University, Allahabad 211002, India

(Received 18 May 1994)

The scalar relativistic version of an accurate first-principles full-potential self-consistent linearized muffin-tin orbital (LMTO) method has been employed for describing the physical properties of the II-VI semiconducting compounds, ZnS, ZnSe, and ZnTe. The presently employed modified version of the LMTO method is quite fast and goes beyond the usual LMTO-ASA (atomic-sphere approximation) method in the sense that it permits a completely general shape of the potential and the charge density. Also, in contrast to LMTO-ASA, the present method is capable of treating distorted lattice structures accurately. The calculated values of the lattice parameters are within 1.5% of the experimental values. The calculated values of the bulk modulus and the elastic constants are in good agreement with the available experimental data. The values of the phonon frequencies at some symmetry points are also in close agreement with the experimental data wherever available.

I. INTRODUCTION

In the last decade, it has been observed that structural and lattice-dynamical properties can be determined *ab initio* with reliable accuracy if one can calculate the electronic energy of the solid as a function of the atomic positions using the usual density-functional theory. Recently, the linear-muffin-tin orbital (LMTO) method has drawn much attention towards its application to the study of the electronic structure of molecules as well as of crystalline solids. The method has several advantages. (i) Only a minimal basis set is required in the method; thus it can be applied to large unit cells with high efficiency. (ii) The method treats all the elements of the Periodic Table in a similar manner. Thus atoms with a large number of core states and metals having predominantly *d* or *f* character can be treated easily. (iii) As the augmentation procedure generates the correct shape of the wave function near the nuclei, it is quite accurate. (iv) The use of atom-centered basis functions for the different values of the angular momentum in the method helps one to have a quite clear physical picture.

Usually in the application of the standard LMTO method, an atomic-sphere approximation (ASA) is used to make it efficient. However, this LMTO-ASA method suffers from several disadvantages. (i) It neglects the symmetry-breaking terms by discarding the nonspherical parts of the electron density. (ii) The method discards the interstitial region by replacing the muffin-tin spheres by space-filling Wigner spheres. (iii) It uses spherical Hankel functions with vanishing kinetic energy.

It has been noted that quite reliable results can be attained by employing a LMTO basis set if all the potential terms are determined accurately. For this the sizes of the atomic spheres are shrunk so as to make them nonoverlapping. The potential matrix elements are then split into two parts, one contribution coming from the atomic spheres and the other from the complicated interstitial

region. The first part, i.e., the atomic-sphere part, is easy to evaluate by expanding it in terms of the usual spherical harmonics. On the other hand, the evaluation of the interstitial contribution is quite difficult and very time consuming if done by standard techniques. Efforts have been made to find an efficient and quick way to determine the interstitial contribution. In the method¹ used in the present work, the interstitial quantities were expanded in terms of spherical Hankel functions. The integrals involved three-center were expressed as linear combinations of two-center integrals by numerical means. These two-center integrals involving Hankel functions can easily be evaluated analytically. The method does not employ plane waves and is thus applicable to periodic as well as nonperiodic systems, which so often need to be treated specially when there occur impurities, defects, and lattice distortions or atomic relaxations.

The present LMTO method is seen to produce the electronic structure, cohesive energy, lattice constants, elastic constants, phonon frequencies, mode Grüneisen parameters, and strain parameters for simple systems like Si, C, etc.^{1,2} Very recently, the method has been successfully applied also for III-V and II-VI semiconducting compounds like AlAs, CdS, GaAs, etc. The influence of structural relaxation of the atoms on the valence-band offset at the lattice-matched interfaces of II-VI and III-V semiconductors ZnTe/GaSb(110) and the lattice-mismatched interface ZnS/ZnSe(001) has been investigated.³ The electronic structure, elastic constants, and frozen-phonon frequencies of the parent superconductor CaCuO₂ of the recently discovered high-*T_c* oxide superconductors have been obtained.⁴ Also, very recently, Hg-based superconductors revealing the highest values of *T_c*'s of 165 K have been investigated.⁵

For detailed information about the method used, we refer to earlier articles.^{1,4,5} The results for the three prototypes of II-VI semiconductors, i.e., ZnS, ZnSe, and ZnTe are presented in Sec. II. The main conclusions are included in Sec. III.

II. CALCULATION AND RESULTS

In the present calculation, the basis employed for making expansions of the products of the LMTO envelopes includes functions with $l \leq 4$ and of energies -0.01 , -1.0 , and -2.3 Ry and with two different decays given by $\lambda^2 = -1$ and -3 Ry. The set will include 50 functions for each atomic sphere. The local-density potential of Hedin and Lundquist⁶ has been employed. An absolute convergence to better than 1.0 mRy/atom is obtained with an *spd* basis of 22 LMTO's for each atom. The number of atoms in the unit cell was taken to be four.

The muffin-tin (MT) spheres were chosen to be slightly smaller than touching each other and the radii for cation and anion in each compound were chosen to be equal. The values of the radii of the atomic spheres for ZnS, ZnSe, and ZnTe were taken as 2.210, 2.315, and 2.493 a.u., respectively. An equal number of empty spheres of sizes equal to the cation and anion were introduced in the vacant interstitial sites present in the zinc-blende structure.

A two-panel calculation was performed for each substance to investigate the important role (usually not appreciated) played by the semicore $3d$ and $4d$ states. In ZnS, in the first panel we consider Zn($4s, 4p, 3d$) and S($3s, 3p, 3d$) as valence states, whereas in the second panel no semicore state is considered. Similarly, in ZnSe, in the first panel Zn($4s, 4p, 3d$) and Se($4s, 4p, 4d$) states are taken as the valence states, and in the second panel Se($3d$) states are assumed to be the semicore states. In ZnTe, in the first panel Zn($4s, 4p, 3d$) and Te($5s, 5p, 5d$) states are taken as the valence states, and in the second panel Te($4d$) states are taken as the semicore states. A set of appropriate (*spd*) states was also included on all the empty spheres. The semicore Se($3d$) and Te($4d$) electrons are thus treated as bands in a way similar to valence electrons. The core electrons are not treated in the frozen-core approximation but are allowed to relax. This means that the core-electron charge density is recalculated in each iteration in the self-consistency loop.

In all the calculations, the relativistic effects have been included. The variation of the total electronic energy with the volume of the crystal V is shown in Figs. 1–3,

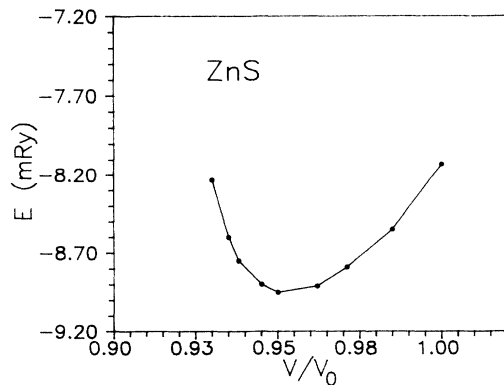


FIG. 1. Variation of crystal energy (mRy) with the ratio of unit-cell volumes. V_0 and V are the experimental and calculated volumes for ZnS.

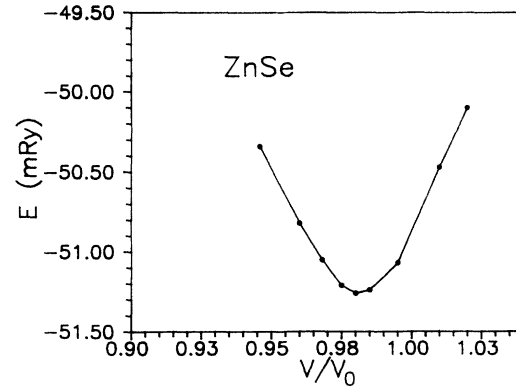


FIG. 2. Same as in Fig. 1 but for ZnSe.

V_0 being the experimental volume of the solid. For ZnS (Fig. 1), the energy minimum appears at a value of lattice parameter (a) equal to 5.318 \AA , which is very close to the experimental value⁷ of 5.409 \AA (see Table I). On the other hand, for ZnSe and ZnTe (see Figs. 2 and 3) the minimum energy appears at $a = 5.633$ and 6.019 \AA , respectively, which are also very near to the experimental values⁷ of 5.668 and 6.101 \AA (see Tables II and III).

The charge outside the muffin-tin sphere, i.e., the difference between the atomic number and the charge lying within the MT sphere for the atoms Zn and S in ZnS is 1.41, and 1.40 electron charges, respectively, for the atoms Zn and Se in ZnSe is 1.22 and 1.68 electron charges, respectively, and for the atoms Zn and Te in ZnTe is 0.88 and 2.27 electron charges, respectively. The total charge per unit cell outside the MT spheres is 2.09e in ZnS, 2.16e in ZnSe, and 2.36e in ZnTe.

A. Electronic structure

The radius of the muffin-tin sphere for the common cation Zn in these Zn-based compounds has been chosen in accordance with the magnitude of the lattice parameter of the solid and it increases from ZnS to ZnTe. The charge inside the MT sphere is seen to decrease with increase in the atomic number of the anion, whereas the re-

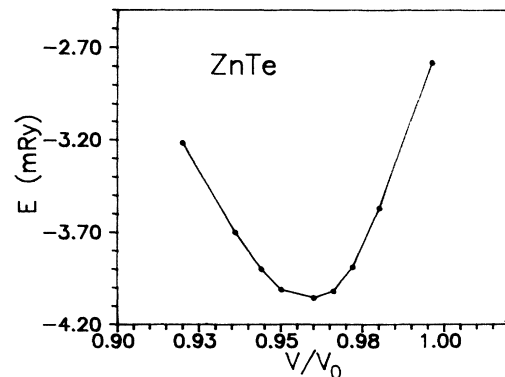


FIG. 3. Same as in Fig. 1 but for ZnTe.

TABLE I. Computed physical quantities for ZnS. The lattice parameter is in Å. The elastic data are in Mbar and the phonon frequencies in cm^{-1} .

| Serial No. | Quantity | Present | Expt. |
|------------|-------------------|---------|--------------------|
| 1 | Lattice parameter | 5.318 | 5.409 ^a |
| 2 | Bulk modulus | 0.852 | 0.767 ^b |
| 3 | C_{11} | 1.220 | 1.000 ^b |
| 4 | C_{12} | 0.667 | 0.650 ^b |
| 5 | C_{44} | 0.378 | 0.340 ^b |
| 6 | TO(Γ) | 289 | 276 ^c |
| 7 | TO(X) | 311 | 316 ^c |
| 8 | TA(X) | 105 | 90 ^c |
| 9 | LA(X_1) | 209 | 211 ^c |
| 10 | LA(X_2) | 299 | |

^aReference 7.

^bReference 11.

^cReference 13.

TABLE II. Computed physical quantities for ZnSe. The lattice parameter is in Å. The elastic data are in Mbar and the phonon frequencies in cm^{-1} .

| Serial No. | Quantity | Present | Expt. |
|------------|-------------------|---------|--------------------|
| 1 | Lattice parameter | 5.633 | 5.668 ^a |
| 2 | Bulk modulus | 0.811 | 0.625 ^b |
| 3 | C_{11} | 1.072 | |
| 4 | C_{12} | 0.675 | |
| 5 | C_{44} | 0.372 | |
| 6 | TO(Γ) | 224 | 213 ^c |
| 7 | TO(X) | 203 | 219 ^c |
| 8 | TA(X) | 79 | 70 ^c |
| 9 | LA(X_1) | 173 | 194 ^c |
| 10 | LA(X_2) | 158 | |

^aReference 7.

^bReference 12.

^cReference 14.

TABLE III. Computed physical quantities for ZnTe. The lattice parameter is in Å. The elastic data are in Mbar and the phonon frequencies in cm^{-1} .

| Serial No. | Quantity | Present | Expt. |
|------------|-------------------|---------|--------------------|
| 1 | Lattice parameter | 6.019 | 6.101 ^a |
| 2 | Bulk modulus | 0.651 | |
| 3 | C_{11} | 0.859 | |
| 4 | C_{12} | 0.547 | |
| 5 | C_{44} | 0.313 | |
| 6 | TO(Γ) | 202 | 177 ^b |
| 7 | TO(X) | 197 | 185 ^b |
| 8 | TA(X) | 73 | 84 ^b |
| 9 | LA(X_1) | 213 | |
| 10 | LA(X_2) | 152 | 136 ^b |

^aReference 7.

^bReference 13.

verse is true for the charges inside the MT spheres of the anions.

The calculated dispersion curves along some important symmetry directions for ZnS, ZnSe, and ZnTe are shown in Figs. 4–6, respectively. The symmetry points are Γ (0,0,0), X (π/a) (1,0,0), K (π/a) (0.75,0.75,0.0), L (π/a) (0.5,0.5,0.5), and W (π/a) (1.0,0.5,0.0).

In ZnS (Fig. 4) at the most symmetric Γ (0,0,0) point, the lowest valence state is a singlet and appears at -13.1 eV, originating from the bonding Zn(4s)-S(3s)-like orbitals. The top of the valence band which has been set at zero energy is formed by the triply degenerate hybridized Zn(4p,3d)-S(3p)-like orbitals in an antibonding manner. The conduction state appearing at 1.85 eV is the antibonding Zn(4s)-S(3s) singlet state. The higher conduction states arise from the hybridization of the Zn(4p,3d)- and S(3p,3d)-like orbitals. The flat bands near -6.0 eV originate from the Zn(3d) states.

At the symmetry point X (π/a) (1,0,0), the lowest singlet valence state has bonding character and is composed of the Zn(4p,3d)-S(3s)-like orbitals. The conduction states are composed of Zn(4p,3d)-S(3s,3d)- and Zn(4s)-S(3p,3d)-like orbitals. No photoemission data for the electronic structure are known to us.

The computed dispersion curves for the electron states in ZnSe are depicted in Fig. 5. At the Γ (0,0,0) symmetry point, similar to ZnS, the lowest valence state at -13.36 eV arises from the bonding Zn(4s)-Se(4s) singlet. The top of the valence band originates from the Zn(4p,3d)-Se(4p)-like orbitals possessing triply degenerate character in an antibonding manner. The bottom of the conduction band appearing at 1.04 eV is comprised of the antibonding 4s states of Zn and Se atoms.

At the X point, the valence states appear either from the Zn(4s,3d)-Se(4p)-like orbitals or from the Zn(4p,3d)-Se(4p)-like orbitals just below the valence-band edge. The semicore Se(3d) states appear much lower, around -47.06 eV.

The computed dispersion curves for the electron states in ZnTe are depicted in Fig. 6. At the Γ (0,0,0) point, similar to the earlier compounds, the lowest valence state at -11.92 eV is the bonding Zn(4s)-Te(5s) singlet. The

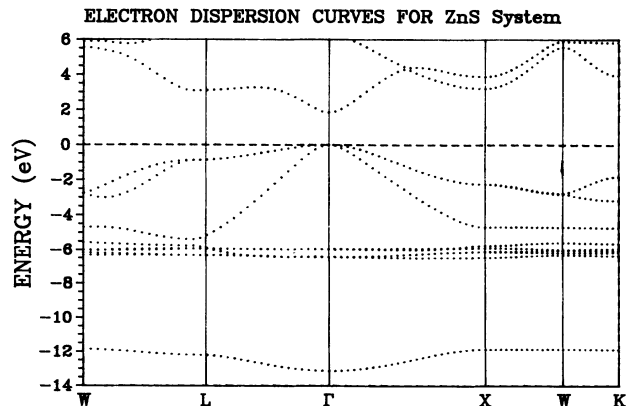


FIG. 4. Dispersion curves for ZnS.

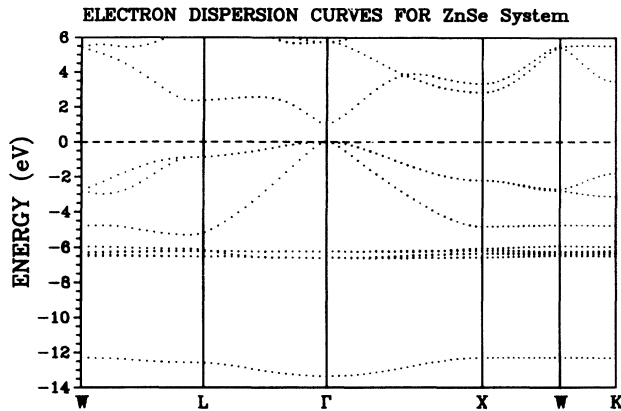


FIG. 5. Dispersion curves for ZnSe.

top of the valence band originates from the $Zn(4p, 3d)$ - $Te(5p)$ -like orbitals possessing triply degenerate character in an antibonding manner. The bottom of the conduction band appearing at 1.00 eV is comprised of the antibonding $4s$ states of Zn and $5s$ states of Te atoms. A triply degenerate state appears in the conduction band at 4.38 eV which is comprised of the $Zn(4p, 3d)$ - $Te(5p, 5d)$ -like orbitals. Again, no experimental data are available for comparison.

At the X point, the lowest singlet valence state has bonding character and is composed of the $Zn(4p, 3d)$ - $Te(5s)$ -like orbitals. The conduction states are composed of $Zn(4s, 4p, 3d)$ - $Te(5s, 5p, 5d)$ -like orbitals. The semicore $Te(4d)$ states appear much lower, around -36.22 eV.

B. Density of states

In the calculation of the electronic density of states (DOS), a sampling method with Gaussian broadening of energy 0.2 eV was employed over a mesh of 19 points in the irreducible part of the Brillouin zone. The calculated DOS for the self-consistent calculation for ZnS is shown in Fig. 7. The valence-band states are distributed over an energy interval of about 13 eV. The low-lying peak near -12.0 eV arises from the hybridized $Zn(4s, 4p, 3d)$ - $S(3s)$ -like orbitals. The other main peaks appearing near -6.0 , -4.6 , and -2.0 eV are comprised of the hybri-

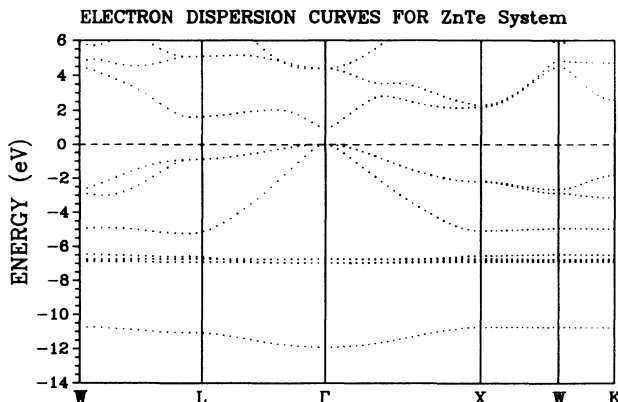


FIG. 6. Dispersion curves for ZnTe.

dized $Zn(4s, 4p, 3d)$ - $S(3p)$ -like orbitals. The top of the valence band is formed by the $4p$ states of Zn and $3p$ states of S. The bottom of the conduction band is formed by the $Zn(4s)$ and $S(3s)$ states. The other main peaks in the conduction band near 4.0 and 6.0 eV originate from the mixed $Zn(4s, 4p)$ - $S(3s, 3p, 3d)$ -like orbitals. The calculated energy gap is direct and its value of 1.85 eV is quite small as compared with the experimental⁷ value of 3.54 eV. Underestimation of electron energy gaps is a usual result of first-principles local-density approximation calculation of the band structures of semiconductors and insulators. This well-known effect is understood as originating from the fact that the eigenvalues of the Kohn-Sham equations are not excitation energies of the system.^{8,9} Accurate band gaps can be obtained from the solution of the quasi-particle equations¹⁰ when the exchange and correlation effects are described by the self-energy which is a nonlocal energy-dependent effective potential. This is beyond the scope of the present work.

The calculated conduction states seem to be reliable in their character although their overall location may be shifted somewhat towards the low-energy side by a magnitude equal to the difference between the experimental and the calculated values of the energy gap. We are not aware of any photoemission data available for ZnS for comparison.

The projected DOS for ZnSe is shown in Fig. 8. The valence-band states appear in an energy interval of 13.36 eV. The major peaks in the valence-state region appearing near -12.5 , -6.36 , -4.75 , and -2.19 eV originate mainly from hybridized $Zn(4s, 4p, 3d)$ - $Se(4s)$ -, $Zn(3d)$ -, $Zn(4s, 3d)$ - $Se(4p)$ -, and $Zn(4p)$ - $Se(4p)$ -like orbitals, respectively. All the peaks in the conduction-band region near 3.01, 3.78, 5.01, and 5.80 eV arise from the mixed $Zn(4s, 4p)$ - $Se(4s, 4p, 4d)$ orbitals. The calculated energy gap of 1.04 eV is quite small as compared to the experimental⁷ value of 2.58 eV.

The projected DOS for ZnTe is shown in Fig. 9. The valence-band states appear in an energy interval of 11.92 eV. The major peaks in the valence-state region appearing near -11.00 , -6.83 , -4.91 , and -2.20 eV arise from mixed $Zn(4s, 4p, 3d)$ - $Te(5s)$ -, $Zn(3d)$ -, $Zn(4s, 4p, 3d)$ - $Te(5p)$ -, and $Zn(4p)$ - $Te(5p)$ -like orbitals, respectively. The peaks in the conduction-band region near 3.0 and 4.5 eV originate from the hybridized $Zn(4s, 4p)$ - $Te(5s, 5p, 5d)$ orbitals. The calculated energy gap of 1.00 eV is quite small as compared to the experimental⁷ value of 2.26 eV.

C. Charge density

Contour plots of the self-consistent valence charge density for ZnS, ZnSe, and ZnTe in the $(1, \bar{1}, 0)$ plane are shown in Figs. 10–12, respectively. The contours are plotted in steps of 0.01 electron/(a.u.)³ up to a maximum of 0.15 $e/(a.u.)^3$.

D. Elastic constants

For the evaluation of the energy derivatives, we have used five different values of ϵ . The maximum value of ϵ is taken as ± 0.04 . The change in the internal energy is

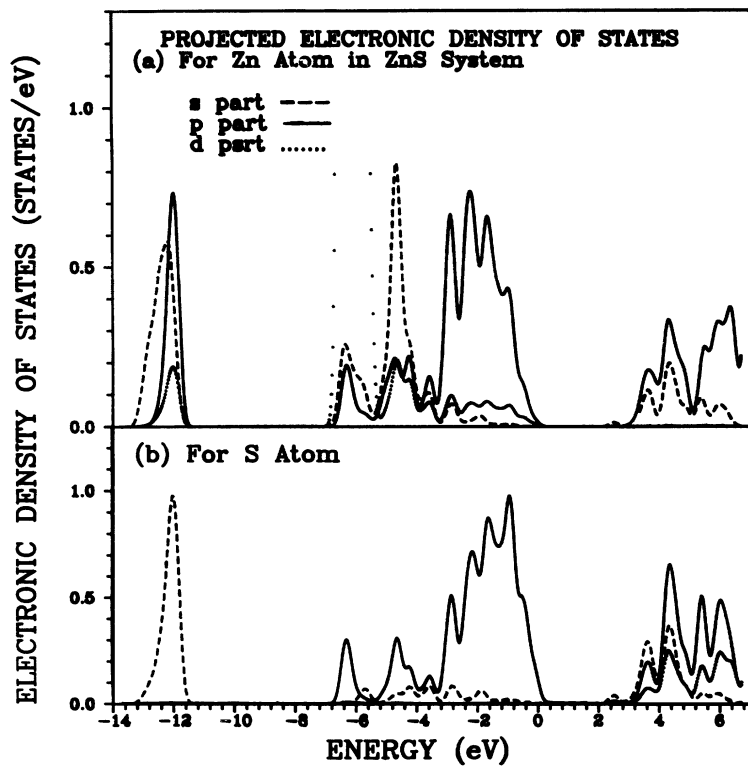


FIG. 7. Projected electronic density of states at different atoms for ZnS.

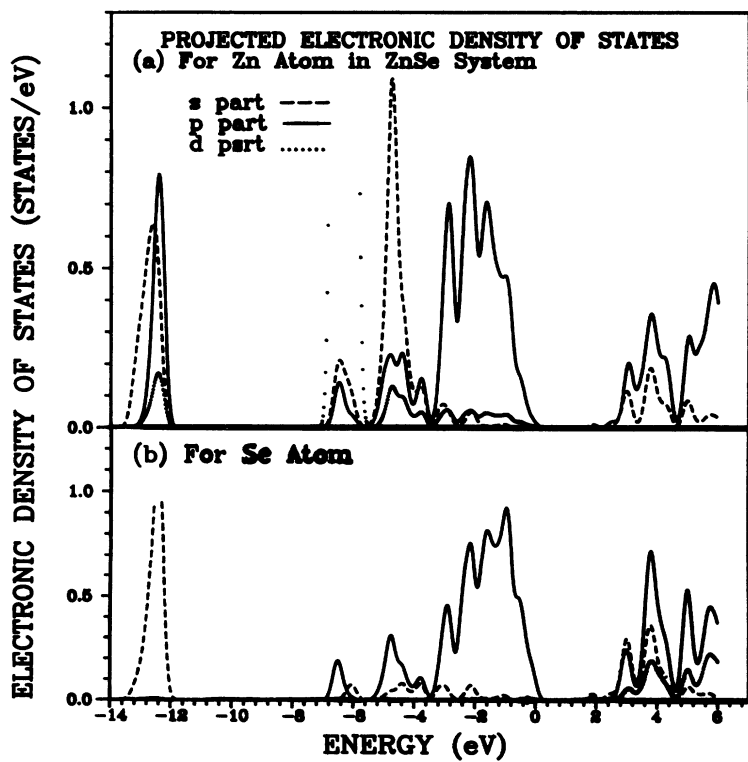


FIG. 8. Projected electronic density of states at different atoms for ZnSe.

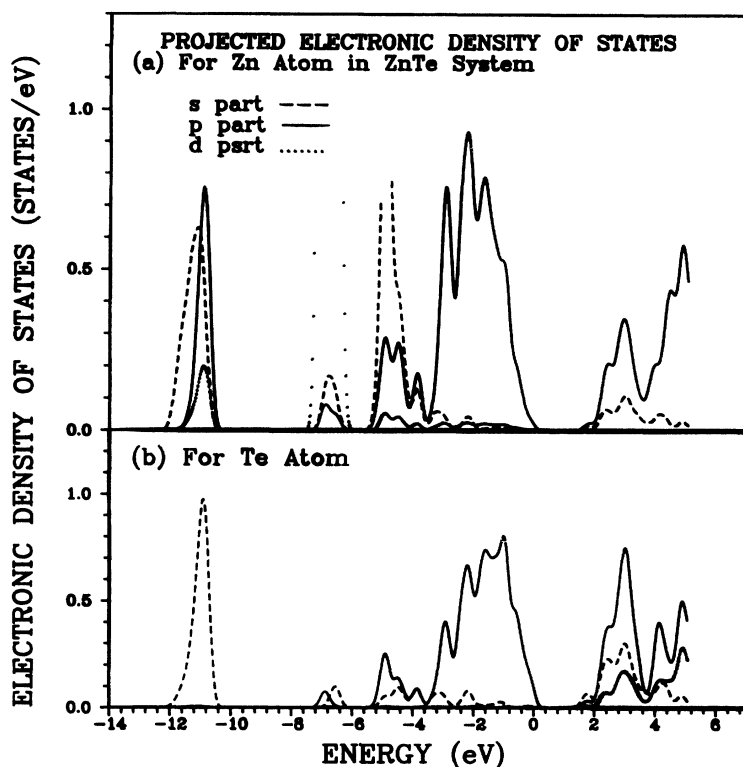


FIG. 9. Projected electronic density of states at different atoms for ZnTe.

fitted to polynomials of order 0, 2, and 3 and the coefficients of the various polynomials are evaluated; they are equal to some multiple of the different combinations of the elastic constants.

The results for the elastic constants for ZnS, ZnSe, and ZnTe are included in Tables I–III, respectively. For ZnS, the presently computed values for the bulk moduli C_{11} and C_{44} are higher than the experimental values.¹¹

The value of C_{12} is in very good agreement with the experimental value, within 2.7% (see Table I). We have also calculated the various elastic constants for the ZnSe and ZnTe systems. However, the experimental results are not available for comparison except for the bulk modulus of ZnSe, which is slightly higher than the experimental value¹² (see Table II).

E. Phonon frequencies

The variation of the internal energy with different types of static deformations in the small-deformation lim-

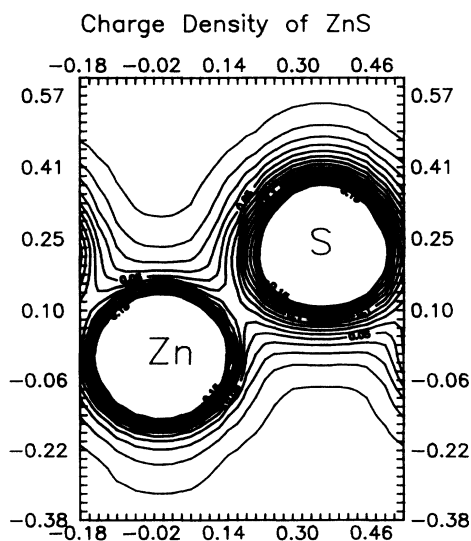


FIG. 10. Contour plots of the self-consistent charge density for the $(1\bar{1}0)$ plane of ZnS. The plots are in steps of 0.01 electron/ $(\text{a.u.})^3$ up to a maximum of $0.15e/(\text{a.u.})^3$.

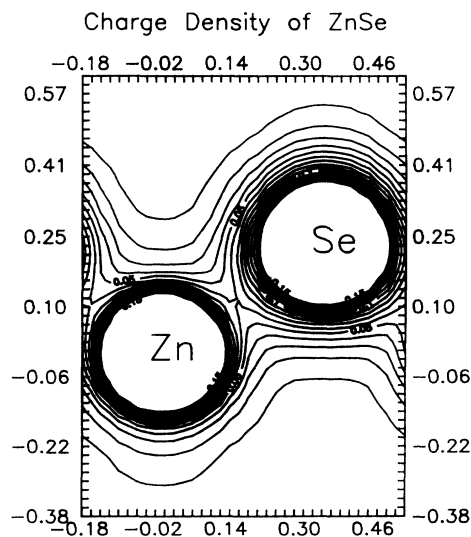


FIG. 11. Same as in Fig. 10 but for ZnSe.

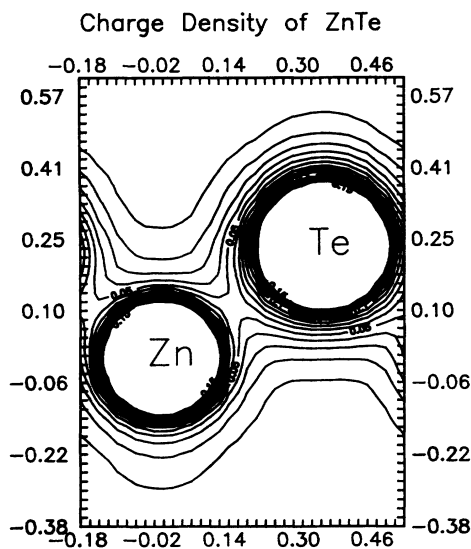


FIG. 12. Same as in Fig. 10 but for ZnTe.

it can be utilized for the determination of some of the frozen symmetry points of the Brillouin zone. Calculations have been performed for the transverse optical (TO) mode at $\mathbf{k}=\mathbf{0}$ (Γ point) and transverse optical, transverse acoustic (TA), and longitudinal acoustic (LA) modes at the point X (π/a) (1,0,0). The transverse optic mode splits because of the motion of the single atom in the mode, each atom possessing different mass. The results for ZnS, ZnSe, and ZnTe have been included in Tables I–III, respectively.

For ZnS, the various calculated phonon frequencies are in close agreement with the experimental data.¹³ The lon-

gitudinal acoustical mode phonon frequency at 209 cm^{-1} is in excellent agreement with the experimental value of 211 cm^{-1} (see Table I). In ZnSe, similarly to the ZnS system, the calculated phonon frequencies are in agreement with the experimental values¹⁴ (see Table II). In the ZnTe system also, the calculated frequencies are in close agreement with the available experimental data.¹³ Keeping in view the complicated distortion involved in these phonon modes and the complexity of the total-energy calculation in the local-density formulation and the inherent uncertainty in measurements, the agreement seems to be satisfactory.

III. CONCLUSIONS

The modified version of the first-principles full-potential self-consistent LMTO method has the capacity to predict most of the physical quantities like the lattice parameter, bulk modulus, elastic constants, phonon frequencies, etc. The method has been employed to compute the various physical quantities of the II-VI semiconducting compounds ZnS, ZnSe, and ZnTe. The computed results for all three systems are in close agreement with the available experimental data.

ACKNOWLEDGMENTS

All the calculations were performed on MicroVax II, HP 720, and DEIL 5100 systems available to us. Financial assistance from the Department of Science and Technology, New Delhi and the University Grants Commission, New Delhi is acknowledged.

¹M. Methfessel, Phys. Rev. B **38**, 1537 (1988).

²M. Methfessel, C. O. Rodriguez, and O. K. Anderson, Phys. Rev. B **40**, 2009 (1989).

³M. Methfessel, Bal K. Agrawal, and M. Scheffler (unpublished).

⁴Bal K. Agrawal and Savitri Agrawal, Phys. Rev. B **45**, 8321 (1992).

⁵Bal K. Agrawal and Savitri Agrawal, Physica C (to be published).

⁶L. Hedin and B. I. Lundquist, J. Phys. C **4**, 2063 (1971).

⁷CRC Handbook of Chemistry and Physics, 70th ed., edited by

R. C. Weast, D. R. Lide, M. J. Astle, and W. H. Beyer, (Chemical Rubber, Boca Raton, 1990), pp. E-106 and E-110.

⁸J. P. Perdew and M. Levy, Phys. Rev. Lett. **51**, 1884 (1983).

⁹L. J. Sham and M. Schluter, Phys. Rev. Lett. **51**, 1888 (1983).

¹⁰R. W. Godby, M. Schluter, and L. J. Sham, Phys. Rev. Lett. **56**, 2415 (1986).

¹¹E. Prince and W. A. Wooster, Acta Crystallogr. **5**, 386 (1951).

¹²B. H. Lee, J. Appl. Phys. **41**, 2982 (1970).

¹³N. Vagelatos, D. Wehe, and J. King (unpublished).

¹⁴B. Hennion *et al.*, Phys. Lett. **36A**, 376 (1971).